Journal of Medicinal Chemistry

Article

Discovery of Bifunctional Oncogenic Target Inhibitors against Allosteric Mitogen-Activated Protein Kinase (MEK1) and Phosphatidylinositol 3-Kinase (PI3K)

Marcian E. Van Dort , Hao Hong , Hanxiao Wang, Charles A. Nino, Rachel L. Lombardi , Avery E. Blanks, Stefanie Galbán, and Brian D Ross

J. Med. Chem., **Just Accepted Manuscript** • DOI: 10.1021/acs.jmedchem.5b01655 • Publication Date (Web): 04 Mar 2016

ACS Publications

Journal of Medicinal Chemistry is published by the American Chemical Society. 1155 Sixteenth Street N.W., Washington, DC 20036

Discovery of Bifunctional Oncogenic Target Inhibitors against Allosteric Mitogen-Activated Protein Kinase (MEK1) and Phosphatidylinositol 3-Kinase (PI3K)

Journal:	*Journal of Medicinal Chemistry*
Manuscript ID	jm-2015-016556.R4
Manuscript Type:	Article
Date Submitted by the Author:	02-Mar-2016
Complete List of Authors:	Van Dort , Marcian; University of Michigan , Radiology Hong , Hao; University of Michigan , Radiology Wang, Hanxiao; University of Michigan , Radiology Nino, Charles ; University of Michigan , Radiology Lombardi , Rachel ; University of Michigan , Radiology Blanks, Avery; University of Michigan , Radiology Galbán, Stefanie ; University of Michigan, Radiology Ross, Brian; University of Michigan, Radiology

Discovery of Bifunctional Oncogenic Target Inhibitors against Allosteric Mitogen-Activated Protein Kinase (MEK1) and Phosphatidylinositol 3-Kinase (PI3K)

Marcian E. Van Dort[†,‡], Hao Hong[†,‡], Hanxiao Wang[†,‡], Charles A. Nino[†,‡], Rachel L. Lombardi[†,‡], Avery E. Blanks[†,‡], Stefanie Galbán[†,‡] and Brian D. Ross[†,‡,ǁ,*]

[†]Center for Molecular Imaging, [‡]Department of Radiology, [ǁ]Department of Biological Chemistry, The University of Michigan Medical School, Ann Arbor, MI 48109

***Corresponding Author**
Brian D. Ross
University of Michigan,
Center for Molecular Imaging
Departments of Radiology and Biological Chemistry
109 Zina Pitcher Place, Ann Arbor MI 48109-2200 USA.
Email: bdross@umich.edu
Phone: 734-763-2099
Fax: 734-763-5447

ABSTRACT

The synthesis of a series of single entity, bifunctional MEK1/PI3K inhibitors achieved by covalent linking of structural analogs of the ATP-competitive PI3K inhibitor ZSTK474 and the ATP-noncompetitive MEK inhibitor PD0325901 is described. Inhibitors displayed potent *in vitro* inhibition of MEK1 ($0.015 < IC_{50}$ (nM) < 56.7) and PI3K ($54 < IC_{50}$ (nM) < 341) in enzymatic inhibition assays. Concurrent MEK1 and PI3K inhibition was demonstrated with inhibitors **9** and **14** in two tumor cell lines (A549, D54). Inhibitors produced dose-dependent decreased cell viability similar to the combined administration of equivalent doses of ZSTK474 and PD0325901. *In vivo* efficacy of **14** following oral administration was demonstrated in a D54 glioma tumor bearing mouse. Compound **14** showed a 95% and 67% inhibition of tumor ERK1/2 and Akt phosphorylation, respectively, at 2 h post-administration by western blot analysis confirming the bioavailability and efficacy of this bifunctional inhibitor strategy towards combined MEK1/PI3K inhibition.

INTRODUCTION

The Ras/MEK/ERK and PI3K/Akt/mTor pathways play a central role in the regulation of normal cell growth, division and differentiation. Dysregulation of these signaling pathways driven by oncogenic mutations/activation leading to elevated kinase activity has been demonstrated in many human cancers including leukemia, melanoma, breast, ovarian, brain, lung and prostate cancer. Strong evidence suggests the existence of a link (feedback loop) and crosstalk between these two signaling cascades leading to redundancy in survival pathways [1-7]. Consequently, monotherapy targeting a single cascade may be insufficient to induce tumor cell death due to drug resistance mechanisms. Additionally, many *in vitro* and *in vivo* studies have shown synergistic outcomes in tumor cell death by simultaneous - inhibition of these two pathways [8-10]. As the Ras/MEK/ERK and PI3K/Akt/mTor pathways are regulated by different mechanisms, simultaneous co-targeting of these pathways is an attractive anticancer strategy. Current approaches towards multi-kinase drug targeting involve drug administration as either (a) two or more therapeutics (drug cocktail) or (b) a polyfunctional multi-targeting single agent therapeutic. Our effort towards development of a bifunctional anticancer therapeutic for –simultaneous inhibition of these two key signaling pathways has focused on the latter approach. Known limitations of the drug cocktail approach include dissimilar toxicity profiles and

pharmacokinetics as well as issues with patient compliance [7-9, 11, 12]. In principle, appropriately designed poly-targeted single agent therapeutics could provide improved efficacy due to simplification of treatment regimen and reduction in the toxicity associated with the combined off-target effects of cocktail drug administration [7, 13, 14]. There have been few reports in the literature concerning bifunctional targeting of MEK and PI3K with single chemical inhibitors. Li and coworkers recently reported on a novel thiazolidine-2,4-dione derivative wherein they demonstrated a correlation of its anti-proliferative activity in U937 and DU154 cancer cells with Raf/MEK/Erk and PI3K pathway inhibition using western blot analysis [15]. Additionally, Park *et al*. reported on a [1,3,4]thiadiazolo[3,2-a]pyrimidin-7-one analog identified by structure-based virtual screening which demonstrates inhibition of MEK1 (IC_{50} = 2.2 μM) as well as PI3K (IC_{50} = 0.3 μM) [16].

In a previous report we presented preliminary biological studies with a prototype single agent MEK/PI3K bifunctional inhibitor (**1**; **Figure 1**) wherein structural analogs of the potent ATP-competitive PI3K inhibitor ZSTK474 and the allosteric Raf/MEK inhibitor RO5126766, respectively, were covalently linked to provide a single chemical entity [7]. Bifunctional inhibitor **1** displayed nanomolar inhibition towards PI3K (IC_{50} = 172 nM) and MEK1 (IC_{50} = 473 nM) in *in vitro* binding assays. In addition, cellular activity studies conducted with **1** in two representative human cancer cell lines (A549, PANC-1) showed almost complete inhibition of Akt phosphorylation at the 5 μM concentration level in both cell types at 1 h exposure by western blot analysis [7]. However, the corresponding inhibition of pErk1/2 activity was significantly lower (35 - 40%) in both cell types at this inhibitor concentration. We hypothesized that the limited inhibition displayed by **1** towards pErk1/2 expression as compared to pAkt was due to its comparatively low MEK affinity. Consequently, the intent of the present study was to develop bifunctional MEK/PI3K inhibitors with improved MEK affinity utilizing alternate high affinity MEK ligands in the hybrid compound structure. Benzhydroxamate ester derivatives, as exemplified by PD0325901 and related analogs (**Figure 2**), have been shown to be potent and selective ATP-noncompetitive inhibitors of MEK [17, 18]. Accordingly, a series of MEK/PI3K bifunctional inhibitors were designed incorporating analogs of the PI3K inhibitor ZSTK474 covalently linked with a variety of spacer groups to MEK inhibitors based on the benzhydroxamate ester template. The synthetic development and preliminary biological evaluation of these bifunctional MEK/PI3K inhibitor analogs are presented in this report.

RESULTS AND DISCUSSION

Bifunctional **MEK/PI3K Inhibitor Design Strategy**. X-ray crystal structure analysis of the murine PI3K Delta-ZSTK474 inhibitor complex reveals a tight binding inhibitor interaction within the ATP-binding pocket [19]. The key interactions which contribute to inhibitor binding in this region have been previously reviewed [7]. In brief, one of the morpholine oxygen atoms of ZSTK474 hydrogen bonds with a valine backbone amide group (VAL828) of the PI3K hinge region while the 1,3,5-triazine moiety functions as an adenosine mimic. Interactions between the lone pair of the imidazole nitrogen and the PI3K conserved LYS779 residue also likely contributes to strong binding [19]. Since the second morpholine group does not appear to interact within the ATP binding region we replaced this functionality with a piperazine group for ease of synthetic attachment of the spacer group bearing the MEK inhibitor.

The X-ray co-crystal structure of MEK with the non-ATP competitive MEK inhibitor PD318088 (a closely related structural analog of PD0325901) has been reported [20]. These studies indicate that PD318088 binds to a unique allosteric hydrophobic pocket which is adjacent to but separate from the Mg-ATP binding site. The key binding features for these benzhydroxamate ester class of inhibitors include H-bonding interactions of both hydroxamate oxygens with Lys97 and a dipolar interaction of the 4-fluorine atom on the A ring with the backbone amide NH's of both Val211 and Ser212. In addition, the iodine moiety on the B ring lodges in a hydrophobic pocket where it makes an electrostatic interaction with the backbone carbonyl of Val127. Furthermore, the B ring itself is also predicted to form hydrophobic interactions within the pocket formed by Ile141, Met143, Val127 and Phe209 [20]. Based on these crystal structure analysis data, a short series of covalently linked structural analogs incorporating the ZSTK474 and benzhydroxamate ester templates were developed for further investigation as bifunctional MEK/PI3K inhibitors. Covalent linker attachment of the MEK inhibitor moiety to the PI3K inhibitor was achieved at the hydroxamate group on the basis of the reported MEK pocket inhibitor interaction data, docking studies and ease of synthetic accessibility considerations. Additionally, key structural features present in the hydroxamate side chain of high affinity MEK inhibitors such as **5a** and PD0316684 were incorporated within the linker portion of the hybrid structures to retain high MEK binding site recognition.

Synthetic Chemistry. Key intermediates **2a**, **2b** and **3** (**Figure 3**) used in the preparation of the target bifunctional inhibitor compounds were synthesized as previously reported [7,21]. MEK1 inhibitor **5** was synthesized by treatment of **3** with (2-aminoxy-ethyl)-carbamic acid *tert*-butyl ester [22] in DMF in the presence of DIEA to give intermediate **4** followed by trifluoroacetic acid catalyzed cleavage of the Boc protecting group (**Figure 3**). The synthesis of inhibitor derivative **7** was conducted as shown in **Scheme 1**. Initially, **2b** was treated with bromoacetyl bromide in the presence of triethylamine to give the corresponding 2-bromoacetamide derivative **6** which was reacted with **5** to give inhibitor analog **7** in 18.5% overall yield. Inhibitor analogs **9** and **11** were obtained from the common piperazine substituted 1,3,5-triazine intermediate **2a** as shown in **Scheme 2**. Triazine **2a** was initially treated with 6-bromohexanoyl chloride in the presence of potassium carbonate to afford the corresponding 6-bromohexanamide analog **8** which provided inhibitor analog **9** in 37% yield following reaction with the MEK inhibitor **5** in refluxing acetonitrile. Inhibitor analog **11** was prepared from **2a** in 27.5% overall yield by a similar approach via the 4-chloro-butanesulfonamide intermediate **10**. Preparation of the pegylated linked bifunctional inhibitor **14** was carried out as shown in **Scheme 3**. Initially, piperazine substituted 1,3,5-triazine intermediate **2a** was heated at reflux with the aminoxy-protected PEG4 tosylate derivative and potassium carbonate in toluene to give intermediate **12** followed by TFA catalyzed removal of the Boc group to give the aminoxy derivative **13**. Subsequent reaction of **13** with the activated ester derivative **3** as described previously afforded **14** in 55% yield.

Virtual Docking of Compound 14 at MEK1 and PI3K Binding Pockets. Compound **14** is predicted to retain many of the binding interactions displayed by the potent MEK1 inhibitor PD318088 within the MEK1 allosteric binding region including key interactions of both hydroxamate oxygens with Lys97, the 4 fluorine atom on the A ring with the backbone NH's of Val211 and Ser212 and the iodine containing B-ring within the hydrophobic pocket (**Figure 4A**). Similarly, compound **14** is also predicted to serve as a PI3K inhibitor as it retains the hydrogen bonding interaction of the morpholine group oxygen with the valine backbone amide NH group (Val828) and the imidazole nitrogen interaction with the Lys779 side chain amine group (**Figure 4B**).

SAR of MEK1 and PI3K Inhibition for Bifunctional Inhibitor Analogs. The *in vitro* MEK1 and PI3K inhibition data for inhibitor analogs are presented in **Table 1**. All analogs in the series

demonstrated significantly high MEK1 inhibition in the low nanomolar to subnanomolar range (0.015 nM < IC_{50} < 56.7 nM). The high degree of observed MEK inhibition as exemplified by analogs **9** and **14** could be due to retention of the key hydroxamate side chain structural elements of the potent MEK1 inhibitors PD0316684 and **5** in the linker portion of the inhibitor structures. The corresponding PI3K inhibitory activity for these series of inhibitors was less pronounced (54 nM < IC_{50} < 341 nM) with compound **7** displaying the highest PI3K inhibition (IC_{50} = 54 nM) in the series. The improved PI3K inhibition of **7** compared to **9** could be due to its extended linker chain length although additional electronic interactions attributed to the amide bond in the linker could also play a role. The similar PI3K potency (191 nM < IC_{50} < 341 nM) displayed by analogs **9**, **11** and **14** also suggests that the nature of the linker attachment at the piperazine nitrogen plays a minor role in influencing PI3K inhibition. The calculated lipophilicities (cLog P) for bifunctional inhibitors were in the range of 4.84 – 5.71 (**Table 1**) approaching the acceptable threshold (cLog P < 5) for oral bioavailability.

Cellular Efficacy and Viability Studies. The *in vitro* MEK1 and PI3K inhibitory activity of these series of compounds were also assessed in cultured tumor cells (D54, A549). Cellular efficacy of MEK1 and PI3K inhibition by inhibitor compounds were measured by changes in phosphorylation of pErk1/2 and pAkt, respectively. A549 (**Figure 5A**) and D54 (**Figure 5B**) cells were treated with inhibitors at the indicated concentrations for 1 h and subjected to western blot analysis. As shown in **Figure 5A**, in cultured A549 cells, all compounds in this series displayed a decrease of phosphorylation of pERK1/2, demonstrating the potent efficacy of these compounds in inhibiting enzymatic activity of MEK1 kinase. Similarly, compounds **7**, **9**, and **14** also showed high potency in inhibiting PI3K activity, as indicated by the low level of pAKT in treated cell samples. Noticeably, all inhibitor analogs also demonstrate significant inhibition of MEK activity in both cell lines which correlates well with the *in vitro* inhibition data (**Table 1**). Both MEK and PI3K inhibition was most pronounced in cell lines treated with compounds **9** and **14** compared to compounds **7** and **11**.

The effect of the series of novel compounds on cell viability was determined using the AlamarBlue assay. A549 and D54 tumor cells were treated with bifunctional inhibitor analogs (compounds **7**, **9**, **11** & **14**), MEK1 inhibitor (PD0325901), PI3K inhibitor (ZSTK474) and a combination of ZSTK474 and PD0325901 at 48 h prior to assay analysis. As shown in **Figure 6**,

all inhibitors produced a dose-dependent decrease in cell viability in both A549 (**Figure 6A**) and D54 (**Figure 6B**) tumor cell lines. In particular, compounds **9** and **14** were similar to or in some cases exceeded the therapeutic effects of individual monotherapies (e.g., PD0325901) by compromised cell viability in both cell lines. Interestingly, compounds **9** and **14** were found to be as effective as the combination of ZSTK474 and PD0325901 in terms of the loss of cellular viability in both cell lines (**Figure 6A, B**). Significantly, compounds **9** and **14** were found to have significant anti-tumor activity which was similar to that of the combination therapy consisting of co-incubation with ZSTK474 and PD0325901 (**Figure 6A, B**).

***In vivo* MEK1 and PI3K Inhibition Activity in Tumor Bearing Mice.** Based on the combination of the *in vitro* inhibition data and cellular efficacy/viability studies, we selected compound **14** for further *in vivo* evaluation. Four athymic nude Foxn1nu mice were used to evaluate oncogenic target modulation activity *in vivo*. Mice bearing flank D54 (n=2) and A549 (n=2) tumors were treated with either vehicle or 375 mg/kg of compound **14** by oral gavage at 2 h prior to sacrifice. Western blot analysis of excised tumor tissue revealed that compound **14** inhibited phosphorylation of ERK1/2 and Akt in both tumor types (**Figure 7**). Furthermore, in another preliminary experiment using compound **9** modulation of ERK1/2 and pAkt levels was also achieved in mouse tumors for both A549 and D54 tumors (data not shown). Overall, taken together, this data clearly demonstrates simultaneous suppression of MEK1/PI3K activity can be achieved both *in vitro* and *in vivo* by the bifunctional inhibitor compounds **9** and **14**.

SUMMARY AND CONCLUSIONS

Upregulation of the Ras/MEK/ERK and PI3K/Akt/mTor signaling cascades in response to growth factor stimulation has been demonstrated in many human cancers. Studies have also shown that MEK inhibition promotes a compensatory activation of PI3K/Akt kinase activity. Accordingly, co-targeting of these two signaling pathways has been recognized as a promising chemotherapeutic strategy in effective cancer treatment. To address this goal, a series of prototype bifunctional MEK/PI3K inhibitors were developed by the covalent linking of structural analogs of the ATP-competitive inhibitor ZSTK474 with the ATP-noncompetitive class of MEK inhibitors as represented by PD0325901 using a variety of spacer groups. All inhibitors demonstrated nanomolar to sub-nanomolar inhibition of MEK1 as well as PI3K kinase activity in *in vitro* enzymatic inhibition assays and a dose-dependent decrease in cell viability in the A549

lung adenocarcinoma and D54 glioma cell lines. Additionally, all inhibitors demonstrated significant inhibition of MEK1 activity in these two cell lines in correlation with demonstrating *in vitro* anticancer activity. Preliminary *in vivo* studies conducted in D54 and A549 tumor-bearing mice with compound **14** after oral administration revealed significant inhibition of MEK1 and PI3K activity at 2h post-administration confirming *in vivo* efficacy towards target modulation. To the best of our knowledge, this work represents the first demonstration of simultaneous *in vivo* inhibition of the Ras/MEK/ERK and PI3K/Akt/mTor pathways using a single chemical entity bifunctional inhibitor.

MATERIALS & METHODS

Chemical syntheses involving air or moisture sensitive reagents and solvents were conducted under a positive pressure of nitrogen in oven-dried glassware. Key compound intermediates 1,3,5-triazine analogs (**2a**, **2b)** [7], and 3,4-difluoro-2-(2-fluoro-4-iodo-phenylamino)-benzoic acid pentafluorophenyl ester [21] (compound **3**) were synthesized as previously reported. 16,16-Dimethyl-15-oxo-3,6,9,12,14-pentaoxa-13-azaheptadecyl 4-methylbenzenesulfonate (*t*-Boc-aminoxy PEG4 tosylate) and 4-chlorobutane-1-sulfonyl chloride were purchased from Broadpharm, San Diego, CA and Enamine Ltd., Monmouth Jct. NJ, respectively. All other chemical reagents and anhydrous solvents were obtained from Aldrich Chemical Co., Milwaukee, WI and used without additional purification. Column chromatography was performed on silica gel 60 (230 – 400 mesh ASTM) purchased from EMD Millipore, Billerica, MA. Thin-layer chromatography (TLC) was performed using Analtech silica gel GF Uniplates (250 micron). TLC plates were visualized after development with either ultraviolet (UV) light or by spraying with phosphomolybdic acid reagent with subsequent heating. ^{1}H NMR spectra were recorded on Varian instruments at 400 and 700 MHz, respectively, in $CDCl_3$ or CD_3OD as solvent with tetramethylsilane (TMS) as internal standard. Chemical shifts (δ) and coupling constants (*J*) are reported in parts per million (ppm) and Hertz (Hz), respectively. High resolution mass spectral analyses were performed at the Department of Chemistry, University of Michigan, using either a VG-70-250-S mass spectrometer for electron impact (EI) and chemical ionization (DCI) modes, a Waters Autospec Ultima instrument with an electrospray interface for electrospray ionization (ESI) mode or a Waters Tofspec-2E run in reflectron mode. HPLC was performed using a Waters Breeze HPLC System (Waters Corporation, Milford, MA) equipped

with a Waters 2487 Dual Wavelength Absorbance Detector. HPLC analysis was conducted at ambient temperature on a Waters XSELECT CSH C-18 column (4.6 x 250 mm), 5 μ particle, with 0.1% TFA in H_2O (A) and 0.1% TFA in CH_3CN (B) solvent mixtures at a flow rate of 1 mL/min with UV absorbance monitored at 254 and 280 nm. HPLC runs were conducted using a 25 min solvent gradient of either 30% B to 90% B (Method I), 60% B to 90% B (Method II) or 10% B to 90% B (Method III). All biologically tested compounds were demonstrated to have > 95% chemical purity by reversed-phase gradient HPLC analysis.

3,4-Difluoro-2-(2-fluoro-4-iodo-phenylamino)-*N*-{2-(*tert*-butoxycarbonylamino)ethoxy} benzamide (4)

A solution of (2-aminoxy-ethyl)-carbamic acid *tert*-butyl ester [22] (0.945 g, 5.36 mmol) in DMF (6 mL) was added in portions to a solution of 3,4-difluoro-2-(2-fluoro-4-iodo-phenylamino)-benzoic acid pentafluorophenyl ester [21] (**3**) (3.0 g, 5.36 mmol) in DMF (6 mL) followed by DIEA (1.38 g, 1.87 mL, 10.7 mmol) and stirred at rt for 18 h. The reaction mixture was concentrated to dryness under reduced pressure, diluted with EtOAc (100 mL) and extracted with brine (2 x 50 mL), H_2O (50 mL), dried ($MgSO_4$) and concentrated under reduced pressure. The crude material was purified by silica gel flash chromatography with a gradient of 30% - 55% EtOAc in hexanes to provide 2.77 g (94%) of the title compound **4** as a white foam. ^{1}H NMR ($CDCl_3$): δ 10.31 (br s, 1H), 8.59 (br s, 1H), 7.41 – 7.38 (m, 2H), 7.31 (d, 1H, J = 8.5 Hz), 6.91 – 6.84 (m, 1H), 6.61 – 6.55 (m, 1H), 5.05 (br s, 1H), 3.93 (m, 2H), 3.43 – 3.39 (m, 2H), 1.45 (s, 9H). HRMS (ESI+): *m/z* calculated for $C_{20}H_{22}N_3F_3IO_4$ [M + H^+]: 552.0602. Found: 552.0594.

3,4-Difluoro-2-(2-fluoro-4-iodo-phenylamino)-*N*-(2-aminoethoxy)benzamide (5)

Trifluoroacetic acid (17.1 g, 11.5 mL, 150 mmol) was added to a cold solution (0 – 5 ^{0}C) of **4** (2.77 g, 5.0 mmol) in CH_2Cl_2 (50 mL) under a nitrogen atmosphere and stirred at this temperature for 3 h. Upon completion of reaction, the mixture was diluted with Et_2O (250 mL) and crushed ice (100 g). The pH of the aqueous solution was adjusted to pH 8 by slow addition of aqueous saturated $NaHCO_3$ and the organic layer separated, dried (Na_2SO_4) and concentrated under reduced pressure. The crude product was flash chromatographed on silica gel with a gradient of 5% - 30% CH_3OH in CH_2Cl_2 containing 1% NH_4OH to give 1.72 g (76%) of the title compound **5** as a white solid. ^{1}H NMR (CD_3OD):δ 7.55 – 7.51 (m, 1H), 7.41 (dd, 1H, J = 10.9,

1.9 Hz), 7.32 (dd, 1H, J = 8.6, 1.0 Hz), 6.99 – 6.92 (m, 1H), 6.57 – 6.51 (m, 1H), 4.05 (t, 2H, J = 5.0 Hz), 3.10 (t, 2H, J = 5.0 Hz). HRMS (ESI+): *m/z* calculated for $C_{15}H_{14}N_3F_3IO_2$ [M + H^+]: 452.0077. Found: 452.0079. HPLC (Method I): t_R = 9.72 min.

2-(Difluoromethyl)-1-[4-(4-morpholinyl)-6-{4-(6-(*N*-bromoacetylamino)hexanoyl)}piperazino)-1,3,5-triazin-2-yl]-1*H*-benzimidazole (6)

A solution of the 1,3,5-triazine analog **2b** (0.265 g, 0.50 mmol) and Et_3N (0.102 g, 142 μL, 1.0 mmol) in CH_2Cl_2 (3 mL) was cooled to 0 ^{0}C using an ice bath and treated dropwise under a nitrogen atmosphere with a solution of bromoacetyl bromide (0.122 g, 53 μL, 0.60 mmol) in CH_2Cl_2 (2 mL). The ice bath was removed and the reaction mixture was allowed to warm to rt and stirred for an additional 3 h. The mixture was diluted with EtOAC (100 mL), the organic layer washed with aqueous 1N HCl (50 mL), aqueous saturated $NaHCO_3$, (50 mL), brine (2 x 50 mL) and dried (Na_2SO_4). The crude product was purified by flash chromatography on silica gel with a gradient of 2% - 8% CH_3OH in CH_2Cl_2 to give 0.26 g (80%) of the title compound **6** as a beige amorphous solid. ^{1}H NMR ($CDCl_3$):δ 8.33 (d, 1H, J = 8.0 Hz), 7.90 (d, 1H, J = 8.0 Hz), 7.55 (t, 1H, J = 53.5 Hz), 7.47 – 7.39 (m, 2H), 6.62 (br s, 1H), 3.88 – 3.74 (m, 16H), 3.60 (m, 2H), 3.35 – 3.30 (m, 2H), 2.42 – 2.39 (m, 2H), 1.75 – 1.68 (m, 2H), 1.62 – 1.57 (m, 2H), 1.46 – 1.38 (m, 2H). HRMS (ESI+): *m/z* calculated for $C_{27}H_{35}N_9BrF_2O_3$ [M + H^+]: 650.2009. Found: 650.1985.

***N*-(2-((2-((6-(4-(4-(2-(difluoromethyl)-1*H*-benzo[*d*]imidazol-1-yl)-6-morpholino-1,3,5-triazin-2-yl)piperazin-1-yl)-6-oxohexyl)amino)-2-oxoethyl)amino)ethoxy)-3,4-difluoro-2-((2-fluoro-4-iodophenyl)amino)benzamide** (Compound **7**)

A solution of the benzhydroxamate analog **5** (0.18 g, 0.40 mmol), anhydrous K_2CO_3 (0.061 g, 0.44 mmol) and sodium iodide (0.066 g, 0.44 mmol) in DMF (3 mL) was treated dropwise with a solution of **6** (0.26 g, 0.40 mmol) in DMF (2 mL) and stirred at rt for 18 h. The mixture was diluted with EtOAC (50 mL), the organic layer washed with brine (2 x 25 mL) and dried (Na_2SO_4). The crude product was purified by flash chromatography on silica gel with a gradient of 5% - 20% CH_3OH in CH_2Cl_2 containing 1% NH_4OH to give 0.098 g (24%) of the title compound **7** as a cream amorphous solid. ^{1}H NMR ($CDCl_3$ + 1 drop CD_3OD):δ 8.33 (d, 1H, J = 7.9 Hz), 7.88 (d, 1H, J = 7.8 Hz), 7.55 (t, 1H, J = 53.5 Hz), 7.47 – 7.40 (m, 3H), 7.35 – 7.25 (m,

2H), 6.79 – 6.76 (m, 1H), 6.52 – 6.50 (m, 1H), 4.09 (m, 2H), 3.90 – 3.71 (m, 16H), 3.58 (m, 2H), 3.34 (s, 2H), 3.20 (m, 2H), 2.93 (m, 2H), 2.37 – 2.16 (m, 4H), 1.61 (m, 2H), 1.49 (m, 2H), 1.33 – 1.26 (m, 2H). HRMS (ESI+): *m/z* calculated for $C_{42}H_{47}N_{12}F_5IO_5$ [M + H^+]: 1021.2752 Found: 1021.2754. HPLC (Method I): t_R = 15.34 min (95.3% chemical purity).

2-(Difluoromethyl)-1-[4-(4-morpholinyl)-6-{4-(6-bromohexanoyl)}piperazino)-1,3,5-triazin-2-yl]-1*H*-benzimidazole (8)

A stirred suspension of the 1,3,5-triazine analog **2a** (0.208 g, 0.5 mmol) and anhydrous K_2CO_3 (0.208 g, 1.5 mmol) in methyl ethyl ketone (3.5 mL) was cooled to 0 - 5 ^{0}C using an ice-bath and treated dropwise under a nitrogen atmosphere with a solution of 6-bromohexanoyl chloride (0.112 g, 81 μL, 0.525 mmol) in MEK (1.5 mL). The ice bath was removed and the reaction mixture was stirred at rt for an additional 3 h. The residue obtained after concentration under reduced pressure was partitioned between aqueous saturated $NaHCO_3$ (100 mL) and EtOAC (100 ml). The organic layer was removed, washed successively with brine (50 mL), H_2O (50 mL) and dried (Na_2SO_4). The crude product was purified by flash chromatography on silica gel with a gradient of 3% - 10% acetone in CH_2Cl_2 to give 0.28 g (96%) of the title compound **8** as a colorless oil. ^{1}H NMR ($CDCl_3$):δ 8.33 (d, 1H, J = 7.8 Hz), 7.90 (d, 1H, J = 7.8 Hz), 7.55 (t, 1H, J = 53.5 Hz), 7.47 – 7.39 (m, 2H), 3.89 - 3.60 (m, 16H), 3.44 (t, 2H, J = 6.6 Hz), 2.41 (m, 2H), 1.95 – 1.88 (m, 2H), 1.76 – 1.68 (m, 2H), 1.57 – 1.49 (m, 2H). HRMS (ESI+): *m/z* calculated for $C_{25}H_{32}N_8BrF_2O_2$ [M + H^+]: 593.1794. Found: 593.1795. HPLC (Method I): t_R = 20.38 min.

***N*-(2-((6-(4-(4-(2-(difluoromethyl)-1*H*-benzo[*d*]imidazol-1-yl)-6-morpholino-1,3,5-triazin-2-yl)piperazin-1-yl)-6-oxohexyl)amino)ethoxy)-3,4-difluoro-2-((2-fluoro-4-iodophenyl)amino)benzamide** (Compound **9**)

A mixture of **8** (0.158 g, 0.27 mmol), benzhydroxamate analog **5** (0.24 g, 0.53 mmol), anhydrous K_2CO_3 (0.042 g, 0.30 mmol) and NaI (0.045 g, 0.30 mmol) in CH_3CN (5 mL) was stirred at reflux for 4 h. The reaction mixture was diluted with EtOAc (100 mL) extracted with brine (100 mL) and dried (Na_2SO_4). The crude product was purified by flash chromatography on silica gel with a gradient of 3% - 20% CH_3OH in CH_2Cl_2 containing 1% NH_4OH to give 0.096 g (37%) of the title compound **9** as a white amorphous powder. ^{1}H NMR ($CDCl_3$):δ 8.32 (d, 1H, J = 7.6 Hz), 7.90 (d, 1H, J = 8.4 Hz), 7.63 (m, 1H), 7.54 (t, 1H, J = 53.5 Hz), 7.46 – 7.38 (m, 2H), 7.33 – 7.25 (m, 2H), 6.78 (m, 1H), 6.51 (m, 1H), 4.27 (m, 2H), 3.88 – 3.41 (m, 16H), 3.14 (m, 2H), 2.88 (m,

2H), 2.24 (m, 2H), 1.66 (m, 2H), 1.54 (m, 2H), 1.31 (m, 2H). HRMS (ESI+): *m/z* calculated for $C_{40}H_{44}N_{11}F_5IO_4$ [M + H^+]: 964.2537. Found: 964.2550. HPLC (Method I): t_R = 15.71 min (96.7% chemical purity).

2-(Difluoromethyl)-1-[4-(4-morpholinyl)-6-{4-(4-chlorobutane-1-sulfonyl)}piperazino)-1,3,5-triazin-2-yl]-1*H*-benzimidazole (10)

A solution of the 1,3,5-triazine analog **2a** (0.208 g, 0.5 mmol) and Et_3N (0.061 g, 84 μL, 0.6 mmol) in CH_2Cl_2 (5 mL) was cooled to 0 - 5 ^{0}C under a nitrogen atmosphere using an ice-bath. A solution of 4-chlorobutane-1-sulfonyl chloride (0.096 g, 70 μL, 0.5 mmol) in CH_2Cl_2 (2 mL) was added dropwise, the ice bath removed and the reaction mixture was stirred at rt for 18 h. The reaction mixture was treated with CH_2Cl_2 (50 mL) and washed successively with brine (2 x 50 mL), H_2O (50 mL) and dried (Na_2SO_4). The crude product was purified by flash chromatography on silica gel with a gradient of 1% - 5% CH_3OH in CH_2Cl_2 containing 1% NH_4OH to give 0.264 g (92%) of the title compound **10** as a white foam. ^{1}H NMR ($CDCl_3$):δ 8.31 (d, 1H, J = 7.6 Hz), 7.90 (d, 1H, J = 8.2 Hz), 7.53 (t, 1H, J = 53.3 Hz), 7.47 – 7.39 (m, 2H), 4.00 (m, 4H), 3.89 (m, 4H), 3.80 (m, 4H), 3.58 (t, 2H, J = 6.0 Hz), 3.40 (m, 4H), 3.00 – 2.96 (m, 2H), 2.05 -1.93 (overlapping m, 4H). HRMS (ESI+): *m/z* calculated for $C_{23}H_{30}N_8ClF_2O_3S$ [M + H^+]: 571.1812. Found: 571.1812.

***N*-(2-((4-((4-(4-(2-(difluoromethyl)-1*H*-benzo[*d*]imidazol-1-yl)-6-morpholino-1,3,5-triazin-2-yl)piperazin-1-yl)sulfonyl)butyl)amino)ethoxy)-3,4-difluoro-2-((2-fluoro-4-iodophenyl)amino)benzamide** (Compound **11**)

A mixture of the 4-chlorobutylsulfonamide analog **10** (0.156 g, 0.273 mmol), benzhydroxamate analog **5** (0.248 g, 0.55 mmol), anhydrous K_2CO_3 (0.042 g, 0.30 mmol) and NaI (0.045 g, 0.30 mmol) in CH_3CN (5 mL) was stirred at reflux for 18 h. The mixture was diluted with $CHCl_3$ (100 mL) extracted with brine (2 x 50 mL) and dried (Na_2SO_4). The crude product was purified by flash chromatography on silica gel with a gradient of 5% - 15% CH_3OH in CH_2Cl_2 containing 1% NH_4OH to give 0.080 g (30%) of the title compound **11** as a white amorphous powder. ^{1}H NMR ($CDCl_3$ + 1 drop CD_3OD):δ 8.30 (d, 1H, J = 7.6 Hz), 7.89 (d, 1H, J = 7.4 Hz), 7.53 (t, 1H, J = 53.3 Hz), 7.47 – 7.26 (m, 5H), 6.81 - 6.79 (m, 1H), 6.52 – 6.51 (m, 1H), 4.15 (m, 2H), 3.96 – 3.79 (m, 12H), 3.32 (m, 4H), 3.00 (m, 2H), 2.88 (m, 2H), 2.77 (m, 2H), 1.86 (m, 2H), 1.72 (m,

2H). HRMS (ESI+): *m/z* calculated for $C_{38}H_{42}N_{11}F_5IO_5S$ [M + H^+]: 986.2050. Found: 986.2043. HPLC (Method III): t_R = 20.09 min (97.9% chemical purity).

2-(Difluoromethyl)-1-[4-(4-morpholinyl)-6-{4-(2-(2-(2-(2-(*tert*-butylcarbonylaminoxy)ethoxy)ethoxy)ethoxy)ethyl}piperazino)-1,3,5-triazin-2-yl]-1*H*-benzimidazole (12)

A mixture of the 1,3,5-triazine analog **2a** (0.52 g, 1.25 mmol), *t*-Boc-aminoxy PEG4 tosylate (0.58 g, 1.25 mmol) and anhydrous K_2CO_3 (0.345 g, 2.5 mmol) in toluene (8 mL) was stirred at reflux for 24 h. The mixture was diluted with CH_2Cl_2 (100 mL) extracted with brine (100 mL), H_2O (100 mL) and dried (Na_2SO_4). The crude product was purified by flash chromatography on silica gel with a gradient of 2% - 5% CH_3OH in $CHCl_3$ containing 1% NH_4OH to give 0.63 g (71%) of the title compound **12** as a pale yellow viscous gum. ^{1}H NMR ($CDCl_3$):δ 8.34 (d, 1H, J = 7.8 Hz), 7.99 (s, 1H), 7.88 (d, 1H, J = 7.8 Hz), 7.58 (t, 1H, J = 53.5 Hz), 7.43 – 7.37 (m, 2H), 4.03 – 4.01 (m,2H), 3.91 – 3.86 (m, 8H), 3.80 – 3.78 (m, 4H), 3.73 – 3.63 (m, 12H), 2.66 (t, 2H, J = 5.6 Hz), 2.61 (m, 4H), 1.47 – 1.48 (m, 9H). HRMS (ESI+): *m/z* calculated for $C_{32}H_{48}N_9F_2O_7$: 708.3639. Found: 708.3636. HPLC (Method I): t_R = 9.76 min.

2-(Difluoromethyl)-1-[4-(4-morpholinyl)-6-{4-(2-(2-(2-(2-aminoxy)ethoxy)ethoxy)ethoxy)ethyl}piperazino)-1,3,5-triazin-2-yl]-1*H*-benzimidazole (13)

A stirred solution of **12** (0.255 g, 0.36 mmol) in CH_2Cl_2 (5 mL) was cooled to 0 ^{0}C with an ice bath and treated dropwise with a solution of TFA (2.5 mL) in CH_2Cl_2 (5 mL). The reaction was stirred at 0 - 5 ^{0}C for an additional 2 h then treated with ice-cold water (100 mL) and the pH of the aqueous layer was adjusted to pH 8 with saturated aqueous $NaHCO_3$. The mixture was extracted twice with EtOAc (100 mL), the organic extract washed successively with brine (100 mL), H_2O (100 mL) and dried (Na_2SO_4). The crude product was purified by flash chromatography on silica gel with a gradient of 2% - 4% CH_3OH in CH_2Cl_2 containing 1% NH_4OH to give 0.18 g (82%) of the title compound **13** as a colorless viscous oil. ^{1}H NMR ($CDCl_3$):δ 8.34 (d, 1H, J = 7.8 Hz), 7.89 (d, 1H, J = 8.0 Hz), 7.58 (t, 1H, J = 53.5 Hz), 7.45 – 7.37 (m, 2H), 5.52 (br s, 2H), 3.89 – 3.69 (m, 14H), 3,67 (m, 12 H), 2.66 (t, 2H, J = 5.5 Hz), 2.60 (m, 4H). HRMS (ESI+): *m/z* calculated for $C_{27}H_{40}N_9F_2O_5$ [M + H^+]: 608.3115. Found: 608.3114. HPLC (Method III): t_R = 10.75 min.

***N*-(2-(2-(2-(2-(4-(4-(2-(difluoromethyl)-1*H*-benzo[*d*]imidazol-1-yl)-6-morpholino-1,3,5-triazin-2-yl)piperazin-1-yl)ethoxy)ethoxy)ethoxy)ethoxy)-3,4-difluoro-2-((2-fluoro-4-iodophenyl)amino)benzamide** (Compound **14**)

A mixture of **13** (0.10 g, 1.64 mmol), pentafluorophenyl ester analog **3** (0.092 g, 1.64 mmol) and DIEA (0.042 g 0.58 μL, 0.33 mmol) in DMF (1 mL) was stirred at rt for 24 h. The mixture was diluted with CH_2Cl_2 (100 mL) extracted with brine (2 x 100 mL) and dried (Na_2SO_4). The crude product was purified by flash chromatography on silica gel with a gradient of 2% - 5% CH_3OH in $CHCl_3$ containing 1% NH_4OH to give 0.088 g (55%) of the title compound **14** as a pale pink crystalline solid. ^{1}H NMR ($CDCl_3$ + 1 drop CD_3OD):δ 8.33 (dd, 1H, J = 7.8, 1.4 Hz), 7.86 (dd, 1H, J = 7.0, 1.5 Hz), 7.58 (t, 1H, J = 53.6 Hz), 7.46 – 7.26 (m, 5H), 6.86 – 6.79 (m, 1H), 6.58 – 6.52 (m, 1H), 4.13 – 4.11 (m, 2H), 3.87 – 3.74 (m, 14H), 3.67 – 3.60 (m, 10H), 2.86 (br s, 1H), 2.64 (t, 2H, J = 5.5 Hz), 2.59 – 2.52 (m, 4H). HRMS (ESI+): *m/z* calculated for $C_{40}H_{45}N_{10}F_5IO_6$ [M + H^+]: 983.2483. Found: 983.2477. HPLC (Method I): t_R = 14.56 min.

***In Vitro* MEK1 Inhibition Assays.** In vitro MEK1 inhibition activity of inhibitor analogs were determined using Kinase-Glo® Luminescent Kinase Assay kits from Promega (Wisconsin, USA) per manufacturer's instructions. Purified MEK1 and inactive Erk2 were purchased from Sigma-Aldrich (St. Louis MO, USA) and Carna Biosciences (Kobe, Japan) respectively. Briefly, series of compound dilutions were added in 96-well plates, followed by MEK1, Erk2 and ATP solutions. Kinase reactions were run at 30 ^{o}C for 30 min. Equal volumes of KinaseGlo solution were then added and reactions were incubated at room temperature for a further 30 min. Bioluminescence signals were acquired with an Envision Multilabel Reader from PerkinElmer. Assays were conducted in triplicate with various inhibitor concentrations each run in duplicate. IC_{50} data were calculated using Graphpad Prism software (version 5.0, La Jolla, CA).

***In Vitro* PI3K Inhibition Assays.** Quantitation of PI3K lipid kinase activity was carried out by Life Technologies (Madison, WI) with purified enzyme using the fluorescence-based Adapta TR-FRET assay protocol. Assays were conducted in triplicate with various inhibitor concentrations (0.1 nM – 10 μM).

Virtual Docking Models of Bifunctional Inhibitor Analogs. Docking models of bifunctional inhibitor analogs were obtained using software from Schrödinger Inc. X-ray crystal structures of

MEK1 (PDB code: 3WIG) and PI3K (PDB code: 2WXK) were prepared using the Protein Preparation Wizard in Maestro (Protein Preparation Wizard, Schrödinger, LLC, New York, NY). The protein structure was then used to generate the receptor grids for docking using OPLS2005 with the binding site defined by the native ligand. The bifunctional inhibitor ligands were built and prepared for docking in Maestro using LigPrep 3.4 (LigPrep, Schrödinger, LLC, New York, NY). The docking procedures were performed using Glide 6.7 in Standard Precision mode with default parameters and no constraints [23].

Cell Culture and Cell Death Assays. A human lung adenocarcinoma epithelial cell line A549, and a glioma cell line D54 were grown in RPMI supplemented with 10% heat-inactivated fetal bovine serum (FBS) and 1% penicillin/streptomycin/glutamine (Gibco, Carlsbad, CA). Cells were grown in a humidified incubator at 37 ℃ with a supply of 5% CO_2. Initial testing of the therapeutic effects of inhibitor compounds were accomplished using cell viability assays. Stock solutions of inhibitor compounds (10 mM)**,** ZSTK474 (representative PI3K inhibitor), PD0325901 (representative MEK inhibitor) were prepared in DMSO and used to make final solutions by serial dilution in RPMI media. Control wells were dosed with media containing 1% DMSO carrier solvent. Cell viability was determined 48 h later using an AlarmarBlue assay (Life Technologies, Carlsbad, CA) according to the manufacturers' instructions. Fluorescence signals were determined with a PerkinElmer EnVision Xcite Multilabel Reader (PerkinElmer, Waltham, MA).

Western Blot Analysis. Cells were seeded in 6-well dishes 24 h prior to treatment and incubated with the respective inhibitor compound solutions for 1 h. Cells were washed with phosphate-buffered saline (PBS) and lysed with NP-40 lysis buffer (1% NP40, 150 mM NaCl, and 25 mM Tris, pH 8.0) supplemented with protease inhibitors (Complete Protease Inhibitor Cocktail, Roche, Basel, Switzerland) and phosphatase inhibitors (PhosSTOP, Roche, Basel, Switzerland). Concentration of protein was determined using Lowry assays (Bio-Rad, Hercules, CA) and equal amounts of whole cell protein lysate were loaded in each lane and resolved using 4 - 12% gradient Bis-Tris gel (Invitrogen, CA). Proteins were transferred to 0.2 μm nitrocellulose membranes (Invitrogen, CA). Membranes were incubated overnight at 4 ^{o}C with primary antibodies after blocking, followed by incubation with appropriate horse radish peroxidase (HRP)-conjugated secondary antibody at room temperature for 1 h. ECL-Plus was

used to detect the activity of peroxidase according to the manufacturer's protocol (Amersham Pharmacia, Uppsala, Sweden). Antibodies raised against phospho-p44/42 MAPK (Erk1/2) (Thr202/Tyr204), pAKT(S473), phospho-p70 S6K and total ERK, AKT antibodies were purchased from Cell Signaling Technology (Beverly MA, USA), and anti-beta actin (conjugated with HRP) was purchased from Abcam (Cambridge, MA, USA). Secondary HRP antibodies were purchased from Jackson ImmunoResearch (St. Louis MO, USA).

***In Vivo* Evaluation of Inhibitor Efficacy.** All animal experiments were approved by the University Committee on the Use and Care of Animals (UCUCA) at the University of Michigan. Five-week-old athymic nude Foxn1nu mice were inoculated subcutaneously with 1×10^6 fully suspended D54 cells into the flanks of two mice and similarly, 2 additional mice were inoculated with A549 cells in the flank. Each injectate contained a total volume of 200 μL cell suspension in 50% RPMI medium mixed with 50% BD Matrigel Basement Membrane Matrix (Becton, Dickinson and Company, East Rutherford, NJ). When tumor volumes reached approximately 150 mm^3 by caliper measurement, mice were deprived of food for 4 h followed by administration with either vehicle [200 μL of DMSO:HPBCD (3:2)] or inhibitor analog (**14**) (375 mg/kg in 200 μL of DMSO:HPBCD (3:2) orally at 2 h prior to sacrifice. Tumor tissues were collected from both vehicle and drug-treated groups and subjected to Western blot analysis as previously described.

Supporting Information

H-1 NMR spectral data for compounds 5 – 14 (PDF); HPLC analysis data for compounds 7, 9, 11, 14 (PDF); Molecular formula strings for compounds 2b, 5 – 14 (CSV).

***Corresponding Author**

Brian D. Ross

University of Michigan,

Center for Molecular Imaging

Departments of Radiology and Biological Chemistry

109 Zina Pitcher Place, Ann Arbor MI 48109-2200 USA.

Email: bdross@umich.edu

Phone: 734-763-2099

Fax: 734-763-5447

Abbreviations Used

Akt, Protein Kinase B; MEK, Allosteric Mitogen-Activated Protein Kinase; PI3K, Phosphatidylinositol 3-Kinase; mTor, mammalian target of rapamycin; br s, broad signal; cLogP, calculated log P; CH_3CN, acetonitrile; DCM, dichloromethane; DMF, *N*,*N*-dimethylformamide; DIEA, *N*,*N*-diisopropylethylamine; DMSO, dimethylsulfoxide; Et_3N, trimethylamine; HPBCD, (2-hydroxypropyl)-beta-cyclodextrin; MEK, methyl ethyl ketone; rt, room temperature; TFA, trifluoroacetic acid; THF, tetrahydrofuran;

Acknowledgement

This work was supported in part by NIH/NCI grant PO1CA085878 and R35CA197701.

REFERENCES

(1) Aksamitiene, E.; Kiyatkin, A.; Kholodenko, B. N. Cross-talk between mitogenic Ras/MAPK and survival PI3K/Akt pathways: a fine balance. *Biochem. Soc. Trans.* **2012**, *40*, 139-146.

(2) Carracedo, A.; Ma, L.; Teruya-Feldstein, J.; Rojo, F.; Salmena, L.; Alimonti, A.; Egia, A.; Sasaki, A. T.; Thomas, G.; Kozma, S. C.; Papa, A.; Nardella, C.; Cantley, L. C.; Baselga, J.; Pandolfi, P. P. Inhibition of mTORC1 leads to MAPK pathway activation through a PI3K-dependent feedback loop in human cancer. *J. Clin. Invest.* **2008**, *118*, 3065-3074.

(3) Castellano, E.; Downward, J. RAS interaction with PI3K: more than just another effector pathway. *Genes Cancer* **2011**, *2*, 261-274.

(4) Chandarlapaty, S. Negative feedback and adaptive resistance to the targeted therapy of cancer. *Cancer Discov.* **2012**, *2*, 311-319.

(5) Guenther, M. K.; Graab, U.; Fulda, S. Synthetic lethal interaction between PI3K/Akt/mTOR and Ras/MEK/ERK pathway inhibition in rhabdomyosarcoma. *Cancer Lett.* **2013**, *337*, 200-209.

(6) Kinkade, C. W.; Castillo-Martin, M.; Puzio-Kuter, A.; Yan, J.; Foster, T. H.; Gao, H.; Sun, Y.; Ouyang, X.; Gerald, W. L.; Cordon-Cardo, C.; Abate-Shen, C. Targeting AKT/mTOR and ERK MAPK signaling inhibits hormone-refractory prostate cancer in a preclinical mouse model. *J. Clin. Invest.* **2008**, *118*, 3051-3064.

(7) Van Dort, M. E.; Galban, S.; Wang, H.; Sebolt-Leopold, J.; Whitehead, C.; Hong, H.; Rehemtulla, A.; Ross, B. D. Dual inhibition of allosteric mitogen-activated protein kinase (MEK) and phosphatidylinositol 3-kinase (PI3K) oncogenic targets with a bifunctional inhibitor. *Bioorg. Med. Chem.* **2015**, *23*, 1386-1394.

(8) Hoeflich, K. P.; Merchant, M.; Orr, C.; Chan, J.; Den Otter, D.; Berry, L.; Kasman, I.; Koeppen, H.; Rice, K.; Yang, N. Y.; Engst, S.; Johnston, S.; Friedman, L. S.; Belvin, M. Intermittent administration of MEK inhibitor GDC-0973 plus PI3K inhibitor GDC-0941 triggers robust apoptosis and tumor growth inhibition. *Cancer Res.* **2012**, *72*, 210-219.

(9) Renshaw, J.; Taylor, K. R.; Bishop, R.; Valenti, M.; De Haven Brandon, A.; Gowan, S.; Eccles, S. A.; Ruddle, R. R.; Johnson, L. D.; Raynaud, F. I.; Selfe, J. L.; Thway, K.; Pietsch, T.; Pearson, A. D.; Shipley, J. Dual blockade of the PI3K/AKT/mTOR (AZD8055) and RAS/MEK/ERK (AZD6244) pathways synergistically inhibits rhabdomyosarcoma cell growth in vitro and in vivo. *Clin. Cancer Res.* **2013**, *19*, 5940-5951.

(10) Williams, T. M.; Flecha, A. R.; Keller, P.; Ram, A.; Karnak, D.; Galban, S.; Galban, C. J.; Ross, B. D.; Lawrence, T. S.; Rehemtulla, A.; Sebolt-Leopold, J. Cotargeting MAPK and PI3K signaling with concurrent radiotherapy as a strategy for the treatment of pancreatic cancer. *Mol. Cancer Ther.* **2012**, *11*, 1193-1202.

(11) Knight, Z. A.; Lin, H.; Shokat, K. M. Targeting the cancer kinome through polypharmacology. *Nat. Rev. Cancer* **2010**, *10*, 130-137.

(12) Zhang, X.; Zhang, J.; Tong, L.; Luo, Y.; Su, M.; Zang, Y.; Li, J.; Lu, W.; Chen, Y. The discovery of colchicine-SAHA hybrids as a new class of antitumor agents. *Bioorg. Med. Chem.* **2013**, *21*, 3240-3244.

(13) Barouch-Bentov, R.; Sauer, K. Mechanisms of drug resistance in kinases. *Expert Opin. Investig. Drugs* **2011**, *20*, 153-208.

(14) Guerrant, W.; Patil, V.; Canzoneri, J. C.; Oyelere, A. K. Dual targeting of histone deacetylase and topoisomerase II with novel bifunctional inhibitors. *J. Med. Chem.* **2012**, *55*, 1465-1477.

(15) Liu, K.; Rao, W.; Parikh, H.; Li, Q.; Guo, T. L.; Grant, S.; Kellogg, G. E.; Zhang, S. 3,5-Disubstituted-thiazolidine-2,4-dione analogs as anticancer agents: design, synthesis and biological characterization. *Eur. J. Med. Chem.* **2012**, *47*, 125-137.

(16) Park, H.; Chien, P. N.; Ryu, S. E. Discovery of potent inhibitors of receptor protein tyrosine phosphatase sigma through the structure-based virtual screening. *Bioorg. Med. Chem. Lett.* **2012**, *22*, 6333-6337.

(17) Barrett, S. D.; Bridges, A. J.; Dudley, D. T.; Saltiel, A. R.; Fergus, J. H.; Flamme, C. M.; Delaney, A. M.; Kaufman, M.; LePage, S.; Leopold, W. R.; Przybranowski, S. A.; Sebolt-Leopold, J.;

Van Becelaere, K.; Doherty, A. M.; Kennedy, R. M.; Marston, D.; Howard, W. A., Jr.; Smith, Y.; Warmus, J. S.; Tecle, H. The discovery of the benzhydroxamate MEK inhibitors CI-1040 and PD 0325901. *Bioorg. Med. Chem. Lett.* **2008**, *18*, 6501-6504.

(18) Sebolt-Leopold, J. S.; Herrera, R. Targeting the mitogen-activated protein kinase cascade to treat cancer. *Nat. Rev. Cancer* **2004**, *4*, 937-947.

(19) Berndt, A.; Miller, S.; Williams, O.; Le, D. D.; Houseman, B. T.; Pacold, J. I.; Gorrec, F.; Hon, W. C.; Liu, Y.; Rommel, C.; Gaillard, P.; Ruckle, T.; Schwarz, M. K.; Shokat, K. M.; Shaw, J. P.; Williams, R. L. The p110 delta structure: mechanisms for selectivity and potency of new PI(3)K inhibitors. *Nat. Chem. Biol.* **2010**, *6*, 117-124.

(20) Ohren, J. F.; Chen, H.; Pavlovsky, A.; Whitehead, C.; Zhang, E.; Kuffa, P.; Yan, C.; McConnell, P.; Spessard, C.; Banotai, C.; Mueller, W. T.; Delaney, A.; Omer, C.; Sebolt-Leopold, J.; Dudley, D. T.; Leung, I. K.; Flamme, C.; Warmus, J.; Kaufman, M.; Barrett, S.; Tecle, H.; Hasemann, C. A. Structures of human MAP kinase kinase 1 (MEK1) and MEK2 describe novel noncompetitive kinase inhibition. *Nat. Struct. Mol. Biol.* **2004**, *11*, 1192-1197.

(21) Barrett, S. D.; Biwersi, C.; Kaufman, M.; Tecle, H.; Warmus, J. S.; Chen, M. H. Oxygenated esters of 4-iodo phenylamino benzhydroxamic acids. WO2002006213A2, 2002.

(22) Ramalingam, K.; Raju, N. Heteroatom-bearing ligands and metal complexes thereof. EP0629617A1, 1997.

(23) Friesner, R. A.; Banks, J. L.; Murphy, R. B.; Halgren, T. A.; Klicic, J. J.; Mainz, D. T.; Repasky, M. P.; Knoll, E. H.; Shelley, M.; Perry, J. K.; Shaw, D. E.; Francis, P.; Shenkin, P. S. Glide: a new approach for rapid, accurate docking and scoring. 1. Method and assessment of docking accuracy. *J. Med. Chem.* **2004**, *47*, 1739-1749.

FIGURE CAPTIONS

Figure 1. Structure and *In Vitro* Enzyme Inhibition Data for First Generation MEK/PI3K Bifunctional Inhibitor **1**

Figure 2. MEK1 Inhibition Activity Data for Benzhydroxamate Analogs.

Figure 3. Key Intermediates used in Synthesis of MEK/PI3K Bifunctional Inhibitors.

Figure 4. Docked structures of compound 14 at MEK1 allosteric pocket and PI3Kα. (A) Binding mode of compound **14** within the MEK1 (PDB code: 3WIG) allosteric catalytic site. The PI3K portion of compound **14** is out to solvent (left). (B) Binding mode of compound **14** to PI3K (PDB code: 2WXK) catalytic site. MEK1 binding portion is out to solvent (left). Atom denotation: grey (carbon); red (oxygen); blue (nitrogen); green (fluorine); white (hydrogen) and purple (iodine). Pi orbital stacking interactions are shown as hashed blue lines while hydrogen bonds are shown as hashed yellow lines.

Figure 5. *In vitro* activity of compounds 7, 9, 11 and 14. Activity of compounds for *in vitro* targeting MAPK/ERK and PI3K/AKT pathways by Western blot analysis of protein lysates obtained from cultured (A) A549 lung tumor and (B) D54 glioma cells. Cells were incubated in the presence of indicated compounds for 1 h and lysates probed with specific antibodies against pAKT and pERK1/2 and compared with vehicle control (DMSO).

Figure 6. Quantification of *in vitro* activity of compounds 7, 9, 11 and 14. Dose dependence of cell viability following exposure to compounds **7**, **9**, **11**, **14** and the PI3K inhibitor ZSTK474 and MEK inhibitor PD0325901 at the indicated concentrations in (A) A549 lung tumor cells and (B) D54 glioma cells. The percentage of viable tumor cells was determined at 24 h following exposure.

Figure 7. Evaluation of compound 14 *in vivo* activity. *In vivo* MEK1 and PI3K inhibition activity in tumor bearing mice. Compound **14** was evaluated in preliminary studies for *in vivo* target modulation. Mice bearing D54 and A549 subcutaneous tumors were treated with either

vehicle or 375 mg/kg of compound **14** by oral gavage at 2 h prior to sacrifice. (A) Western blot analysis of excised tumor tissue showed that compound **14** successfully modulated both MEK1 and PI3K activities in a D54 tumor relative to vehicle control. (B) Western blot analysis of excised A549 tumor tissue showed that compound **14** successfully modulated both MEK1 and PI3K activities in A549 tumor relative to vehicle control. This data demonstrates *in vivo* bioavailability and efficacy of compound **14** for suppression of MEK1/PI3K kinase activities *in vivo* in solid tumors confirming that simultaneous *in vivo* inhibition of the Ras/MEK/ERK and PI3K/Akt/mTor pathways using a single chemical entity bifunctional inhibitor (compound **14**) could be achieved.

Table 1. *In vitro* MEK1 and PI3K Enzyme Inhibition Data

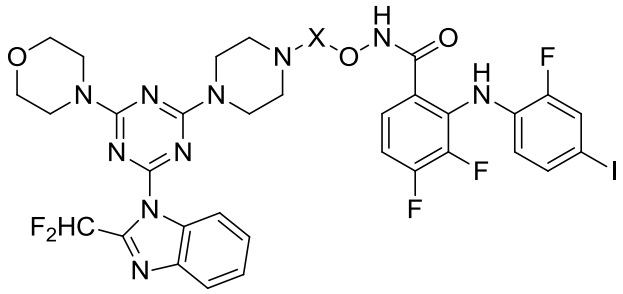

			IC_{50} (nM)[#]	
Compound	**Linker (X)**	**cLogP**	**MEK1**	**PI3K**
7	—C(=O)—$(CH)_5NHCOCH_2NHCH_2CH_2$-	4.84	0.50 ± 1.2	54 ± 25
9	—C(=O)—$(CH)_5NHCH_2CH_2$—	5.58	0.019 ± 3.09	341 ± 56
11	—S(=O)(=O)—$(CH)_4NHCH_2CH_2$—	5.48	56.7 ± 1.3	285 ± 36
14	—$(CH_2CH_2O)_3CH_2CH_2$—	5.71	0.015 ± 1.57	191 ± 64
5	n.a.	3.75	0.00715 ± 1.40	n.d.
PD0316684	n.a.	3.68	13.0 ± 1.6	n.d.
PD0325901	n.a.	2.85	15.0 ± 1.3	n.d.

[#] Binding data are the average of 3 experiments each conducted in duplicate

† cLogP data were obtained using ChemDraw Professional (version 15.0.0.106)

SCHEME 1

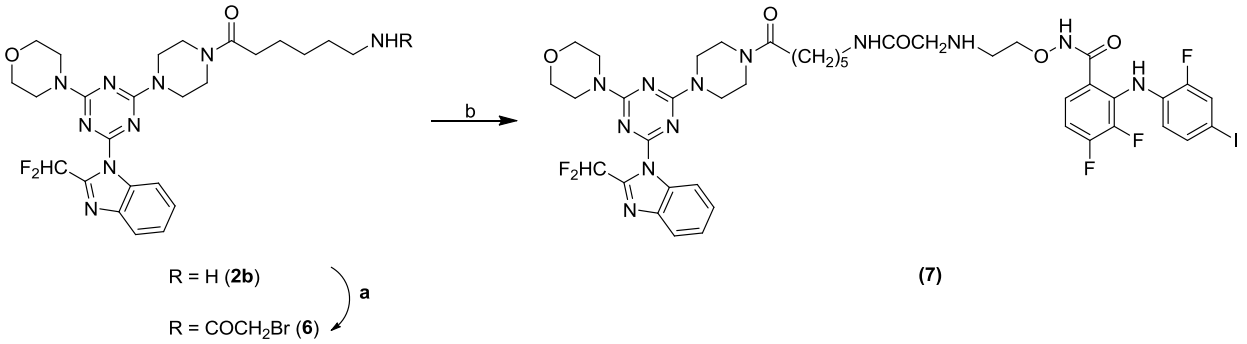

Reagents and conditions: (a) $BrCH_2COBr$, Et_3N, CH_2Cl_2, 0 ^{0}C - rt, 3 h, 80%; (b) **5**, NaI, K_2CO_3, DMF, rt, 4 h, 24%.

SCHEME 2

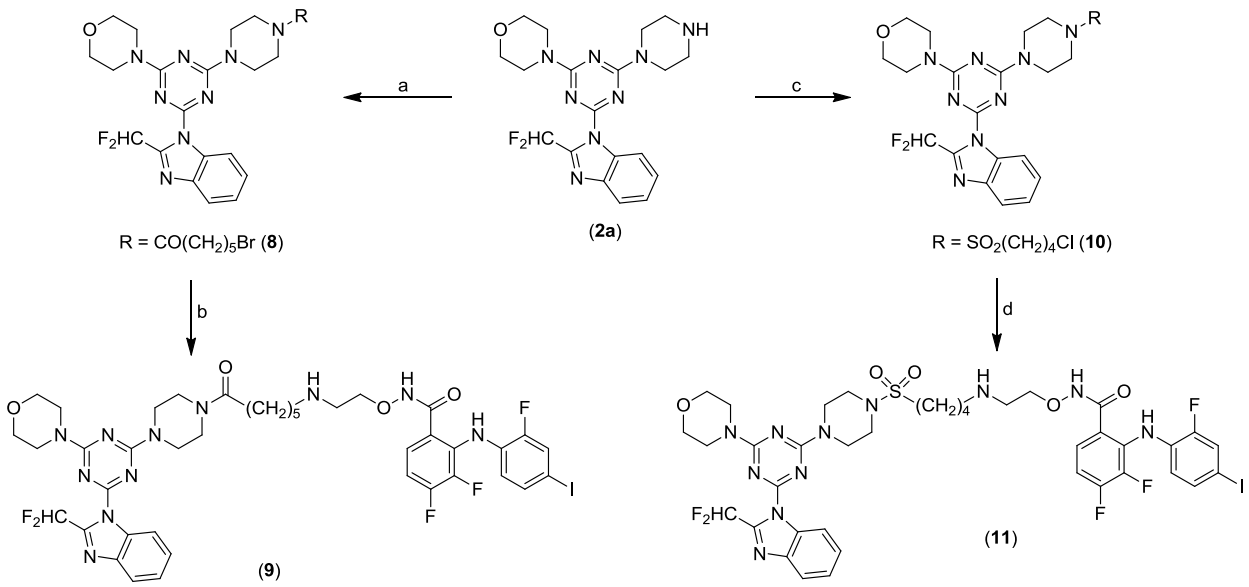

Reagents and conditions: (a) $Br(CH_2)_5COCl$, K_2CO_3, MEK, 0 ^{0}C - rt, 3 h, 96%; (b) **5**, NaI, K_2CO_3, CH_3CN, reflux, 4 h, 37%; (c) $Cl(CH_2)_4SO_2Cl$, Et_3N, CH_2Cl_2, 0 ^{0}C - rt, 18 h, 92%; (d) **5**, NaI, K_2CO_3, CH_3CN, reflux, 18 h, 30%.

SCHEME 3

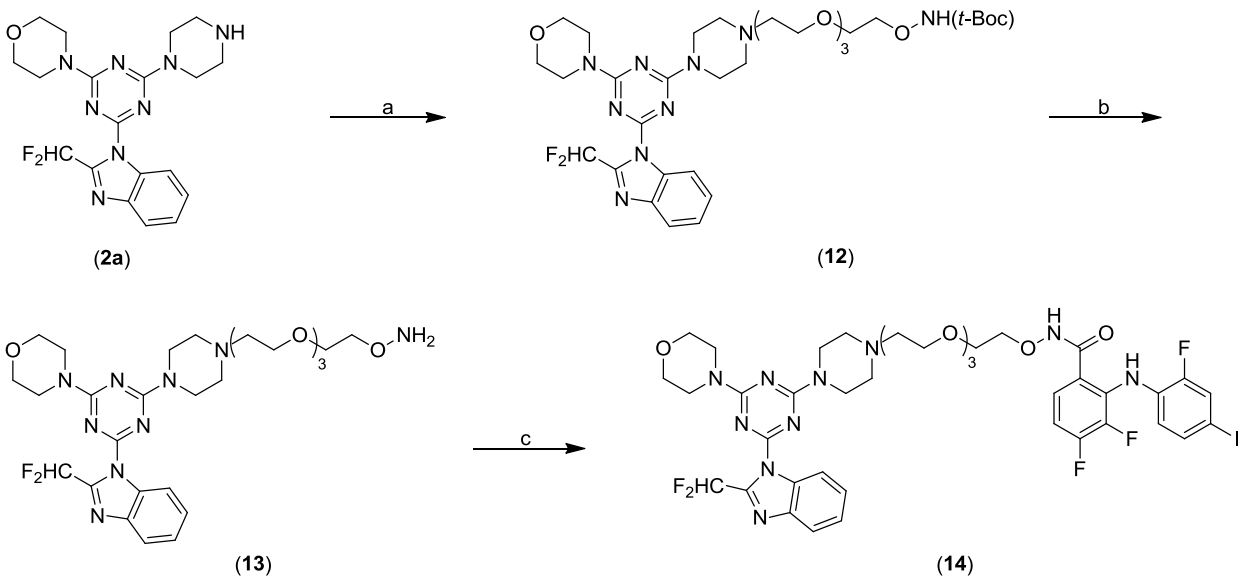

Reagents and conditions: (a) TosO-$(CH_2CH_2O)_4$NH(*t*-Boc), K_2CO_3, toluene, reflux, 24 h, 71%; (b) TFA, CH_2Cl_2, 0 - 5 ^{0}C, 2 h, 82%; (c) **3**, DIEA, DMF, rt, 18 h, 55%.

Figure 1

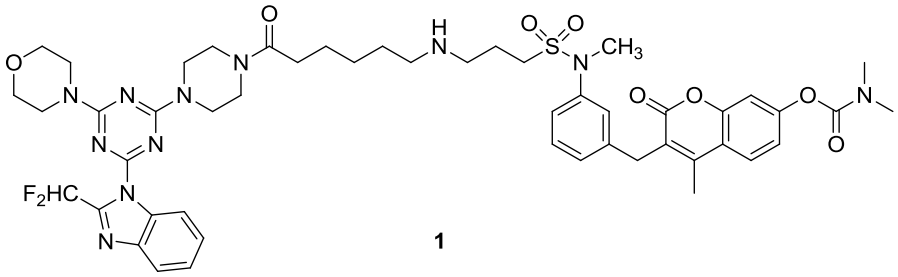

1

IC_{50} (nM)	
PI3K	MEK1
172 ± 24	473 ± 17.8

Figure 2

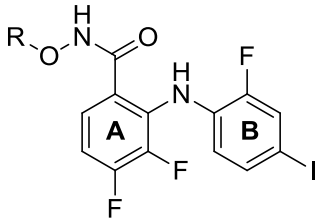

COMPOUND	R	IC_{50} (nM)
PD0325901	*R*-(-)-$CH_2CHOH(CH_2OH)$	0.33[a]
PD0316684	-CH_2CH_2OH	0.07[a]
5a	-$CH_2CH_2NHCH_3$	20[b]

[a] data from reference 17

[b] data from reference 21

Figure 3

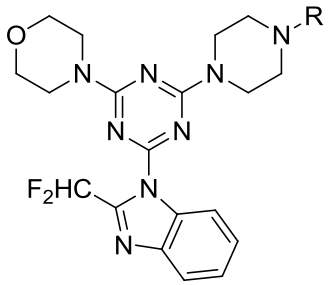

R = H; **(2a)**

R = —C(=O)—$(CH_2)_5NH_2$ **(2b)**

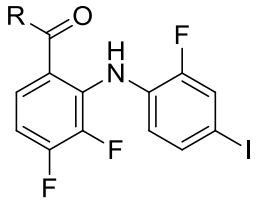

R = C_6F_5O- **(3)**

R = (*t*-Boc)$NHCH_2CH_2ONH$- **(4)**

R = $NH_2CH_2CH_2ONH$- **(5)**

Figure 4

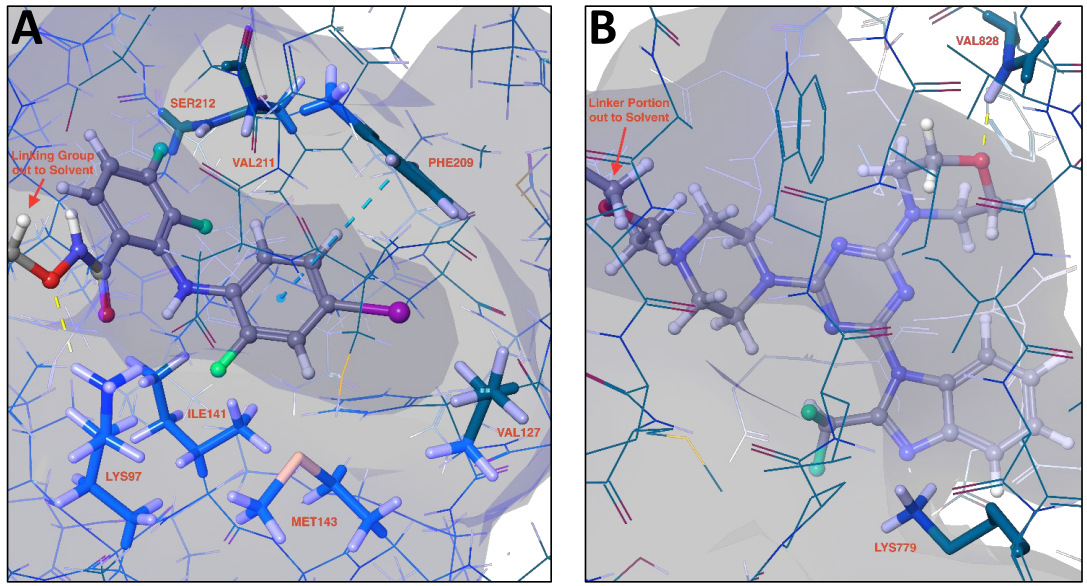

ACS Paragon Plus Environment

Figure 5

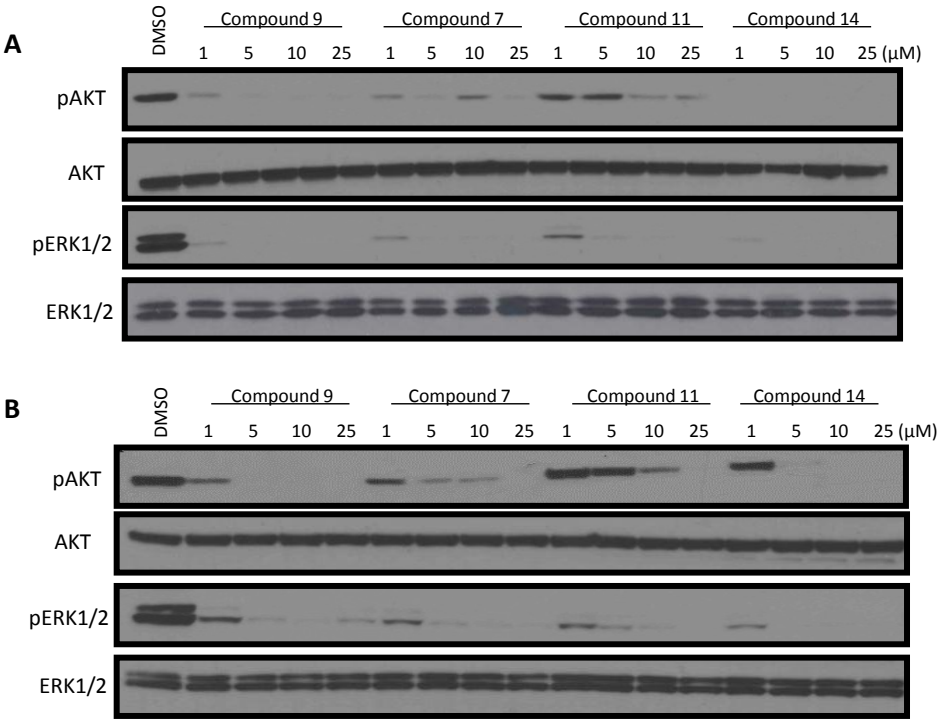
A
DMSO
Compound 9
Compound 7
Compound 11
Compound 14
1 5 10 25 1 5 10 25 1 5 10 25 1 5 10 25 (μM)
pAKT
AKT
pERK1/2
ERK1/2
B
DMSO
Compound 9
Compound 7
Compound 11
Compound 14
1 5 10 25 1 5 10 25 1 5 10 25 1 5 10 25 (μM)
pAKT
AKT
pERK1/2
ERK1/2

Figure 6

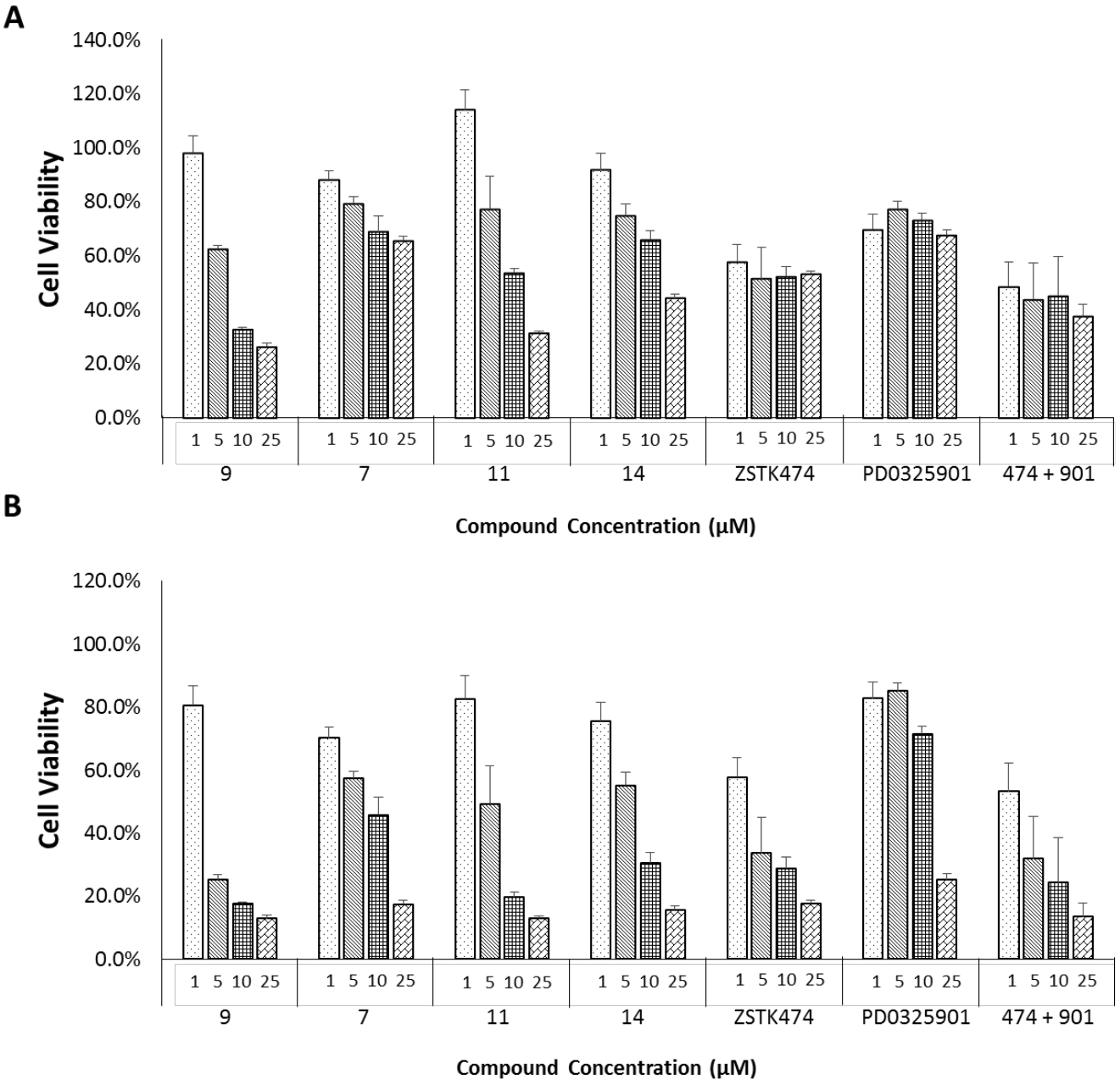
A
Cell Viability
140.0%
120.0%
100.0%
80.0%
60.0%
40.0%
20.0%
0.0%
1 5 10 25
9
7
11
14
ZSTK474
PD0325901
474 + 901
Compound Concentration (μM)
B
Cell Viability
120.0%
100.0%
80.0%
60.0%
40.0%
20.0%
0.0%
1 5 10 25
9
7
11
14
ZSTK474
PD0325901
474 + 901
Compound Concentration (μM)

Figure 7

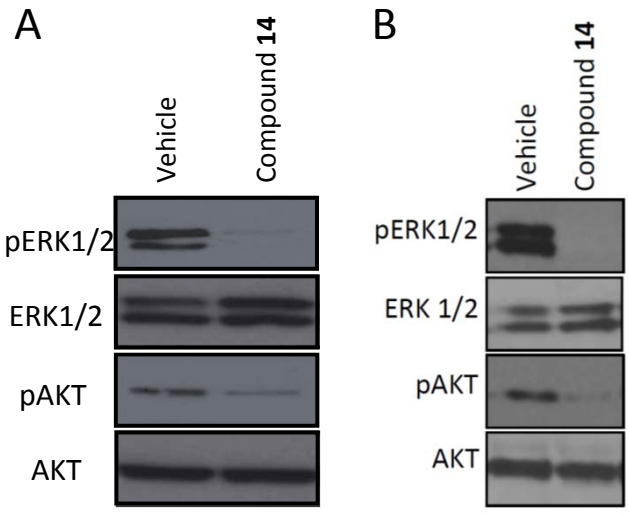
A
Vehicle
Compound 14
pERK1/2
ERK1/2
pAKT
AKT
B
Vehicle
Compound 14
pERK1/2
ERK 1/2
pAKT
AKT

Figure 1

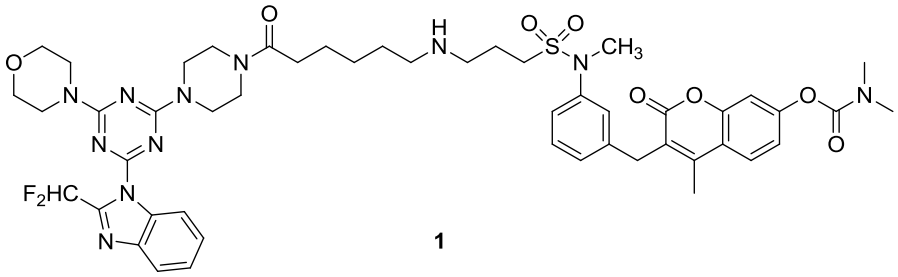

1

IC_{50} (nM)	
PI3K	MEK1
172 ± 24	473 ± 17.8

Table of Contents Graphic

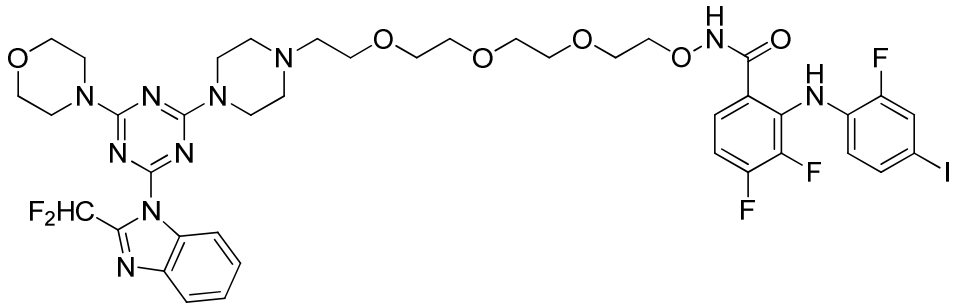

14

MEK1 IC_{50}: 0.015 nM

PI3K IC_{50}: 191 nM

Table 1. *In vitro* MEK1 and PI3K Enzyme Inhibition Data

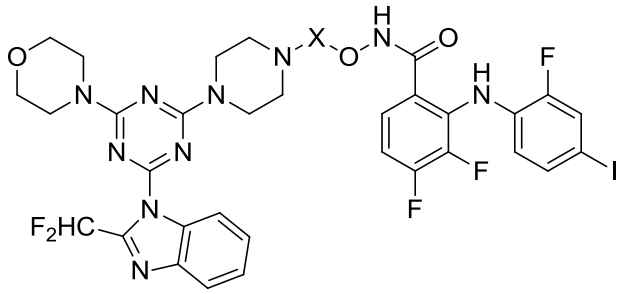

			IC_{50} (nM)[#]	
Compound	**Linker (X)**	**cLogP**	**MEK1**	**PI3K**
7	—C(=O)—$(CH)_5NHCOCH_2NHCH_2CH_2$-	4.84	0.50 ± 1.2	54 ± 25
9	—C(=O)—$(CH)_5NHCH_2CH_2$—	5.58	0.019 ± 3.09	341 ± 56
11	—S(=O)(=O)—$(CH)_4NHCH_2CH_2$—	5.48	56.7 ± 1.3	285 ± 36
14	—$(CH_2CH_2O)_3CH_2CH_2$—	5.71	0.015 ± 1.57	191 ± 64
5	n.a.	3.75	0.00715 ± 1.40	n.d.
PD0316684	n.a.	3.68	13.0 ± 1.6	n.d.
PD0325901	n.a.	2.85	15.0 ± 1.3	n.d.

[#] Binding data are the average of 3 experiments each conducted in duplicate

† cLogP data were obtained using ChemDraw Professional (version 15.0.0.106)

SCHEME 1

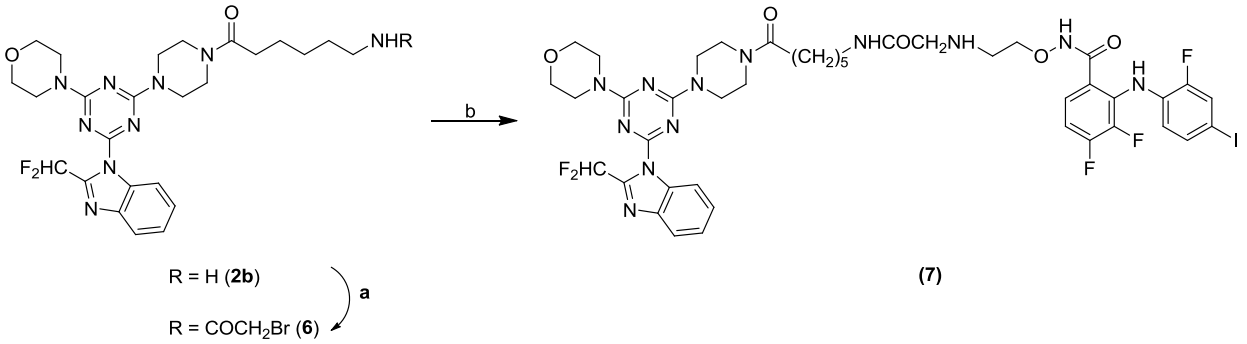

Reagents and conditions: (a) $BrCH_2COBr$, Et_3N, CH_2Cl_2, 0 ^{0}C - rt, 3 h, 80%; (b) **5**, NaI, K_2CO_3, DMF, rt, 4 h, 24%.

SCHEME 2

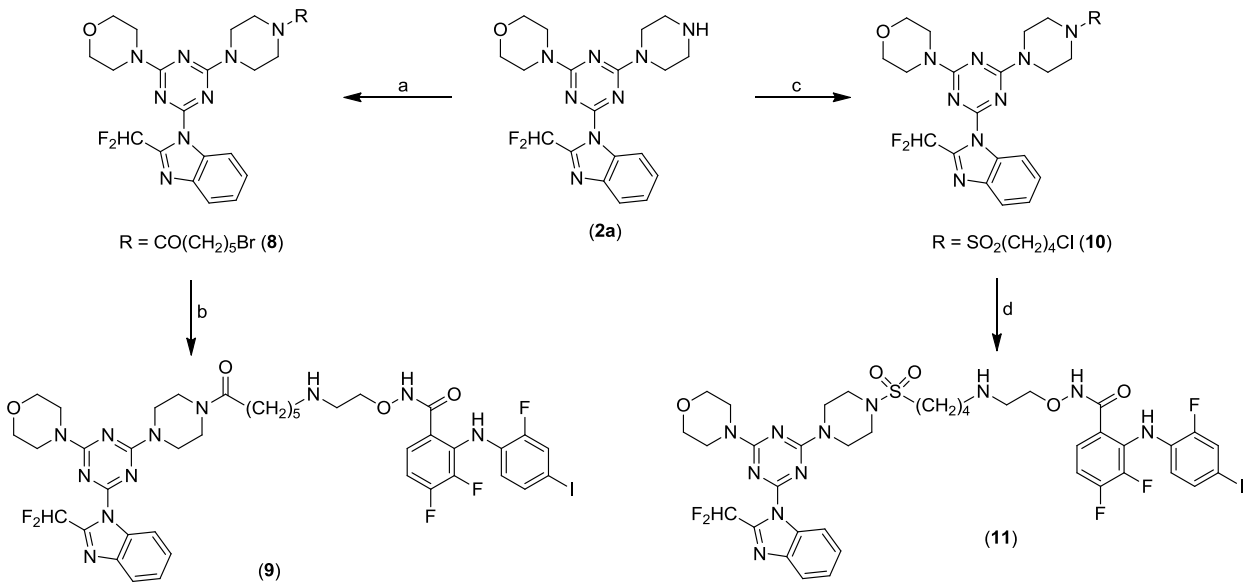

Reagents and conditions: (a) $Br(CH_2)_5COCl$, K_2CO_3, MEK, 0 ^{0}C - rt, 3 h, 96%; (b) **5**, NaI, K_2CO_3, CH_3CN, reflux, 4 h, 37%; (c) $Cl(CH_2)_4SO_2Cl$, Et_3N, CH_2Cl_2, 0 ^{0}C - rt, 18 h, 92%; (d) **5**, NaI, K_2CO_3, CH_3CN, reflux, 18 h, 30%.

SCHEME 3

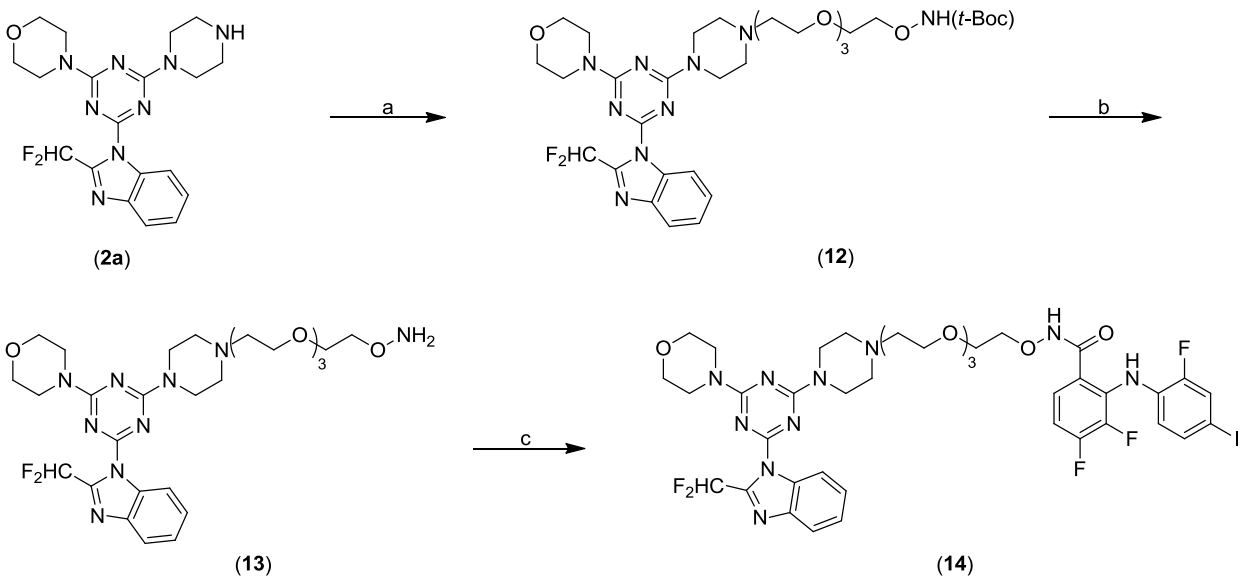

Reagents and conditions: (a) TosO-$(CH_2CH_2O)_4$NH(*t*-Boc), K_2CO_3, toluene, reflux, 24 h, 71%; (b) TFA, CH_2Cl_2, 0 - 5 ^{0}C, 2 h, 82%; (c) **3**, DIEA, DMF, rt, 18 h, 55%.

Figure 1

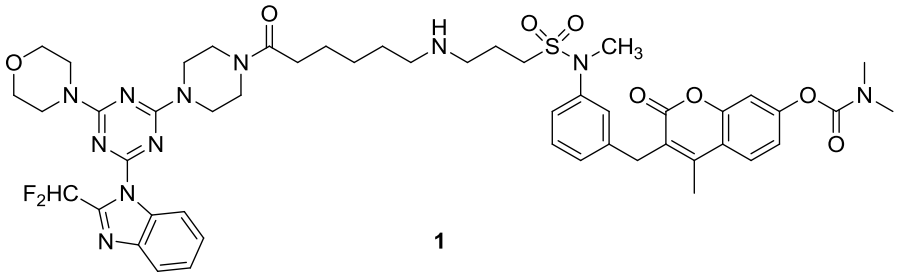

1

IC_{50} (nM)	
PI3K	MEK1
172 ± 24	473 ± 17.8

Figure 2

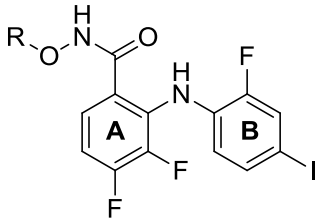

COMPOUND	R	IC_{50} (nM)
PD0325901	*R*-(-)-$CH_2CHOH(CH_2OH)$	0.33[a]
PD0316684	-CH_2CH_2OH	0.07[a]
5a	-$CH_2CH_2NHCH_3$	20[b]

[a] data from reference 17

[b] data from reference 21

Figure 3

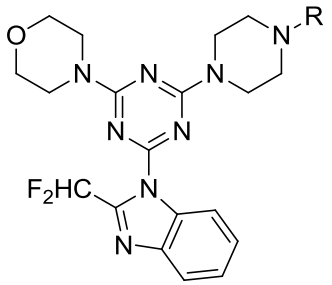

R = H; **(2a)**

R = —C(=O)—$(CH_2)_5NH_2$ **(2b)**

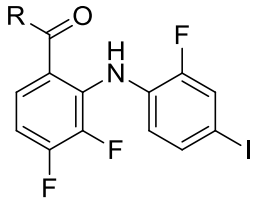

R = C_6F_5O- **(3)**

R = (t-Boc)$NHCH_2CH_2ONH$- **(4)**

R = $NH_2CH_2CH_2ONH$- **(5)**

Figure 4

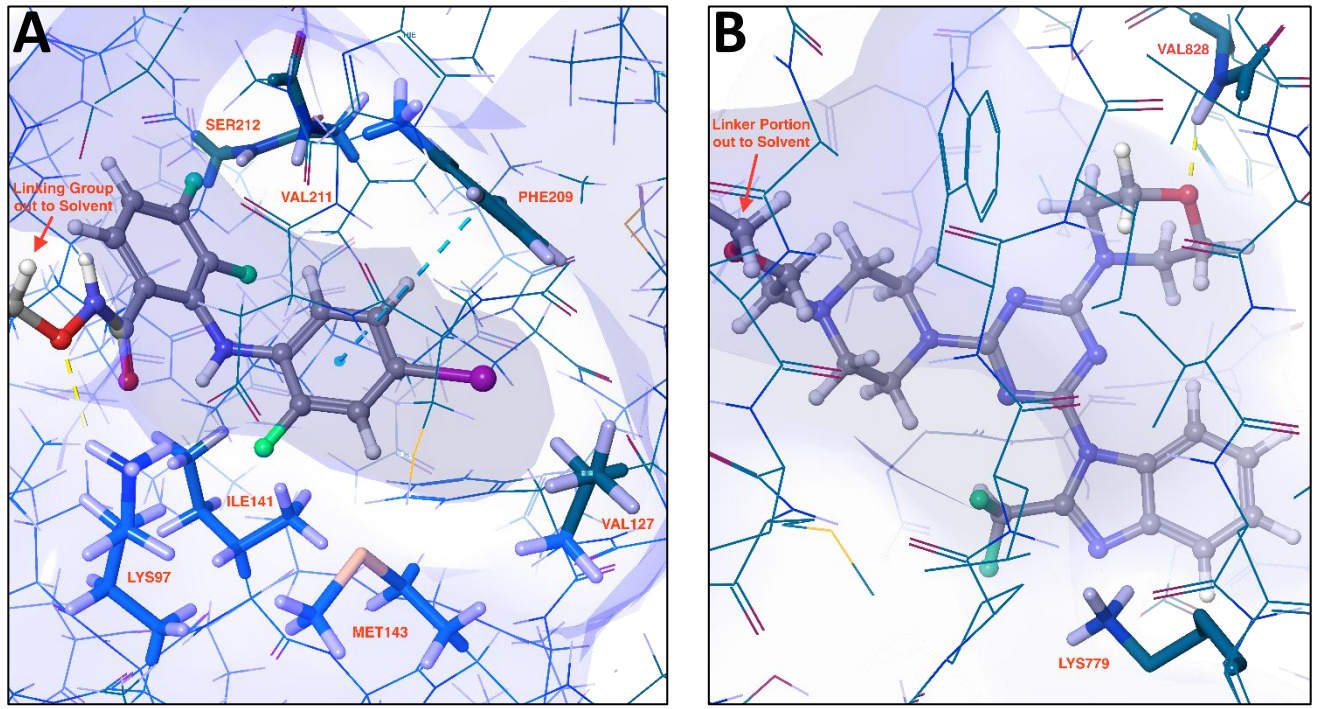
A
SER212
VAL211
PHE209
Linking Group
out to Solvent
ILE141
VAL127
LYS97
MET143
B
VAL828
Linker Portion
out to Solvent
LYS779

Figure 5

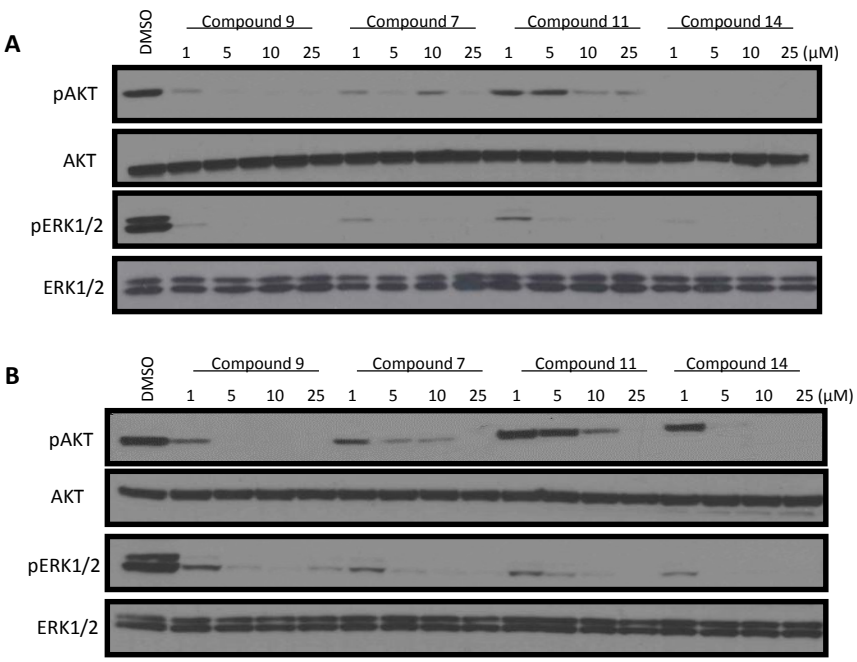
A
DMSO
Compound 9
Compound 7
Compound 11
Compound 14
1 5 10 25 1 5 10 25 1 5 10 25 1 5 10 25 (μM)
pAKT
AKT
pERK1/2
ERK1/2
B
DMSO
Compound 9
Compound 7
Compound 11
Compound 14
1 5 10 25 1 5 10 25 1 5 10 25 1 5 10 25 (μM)
pAKT
AKT
pERK1/2
ERK1/2

Figure 6

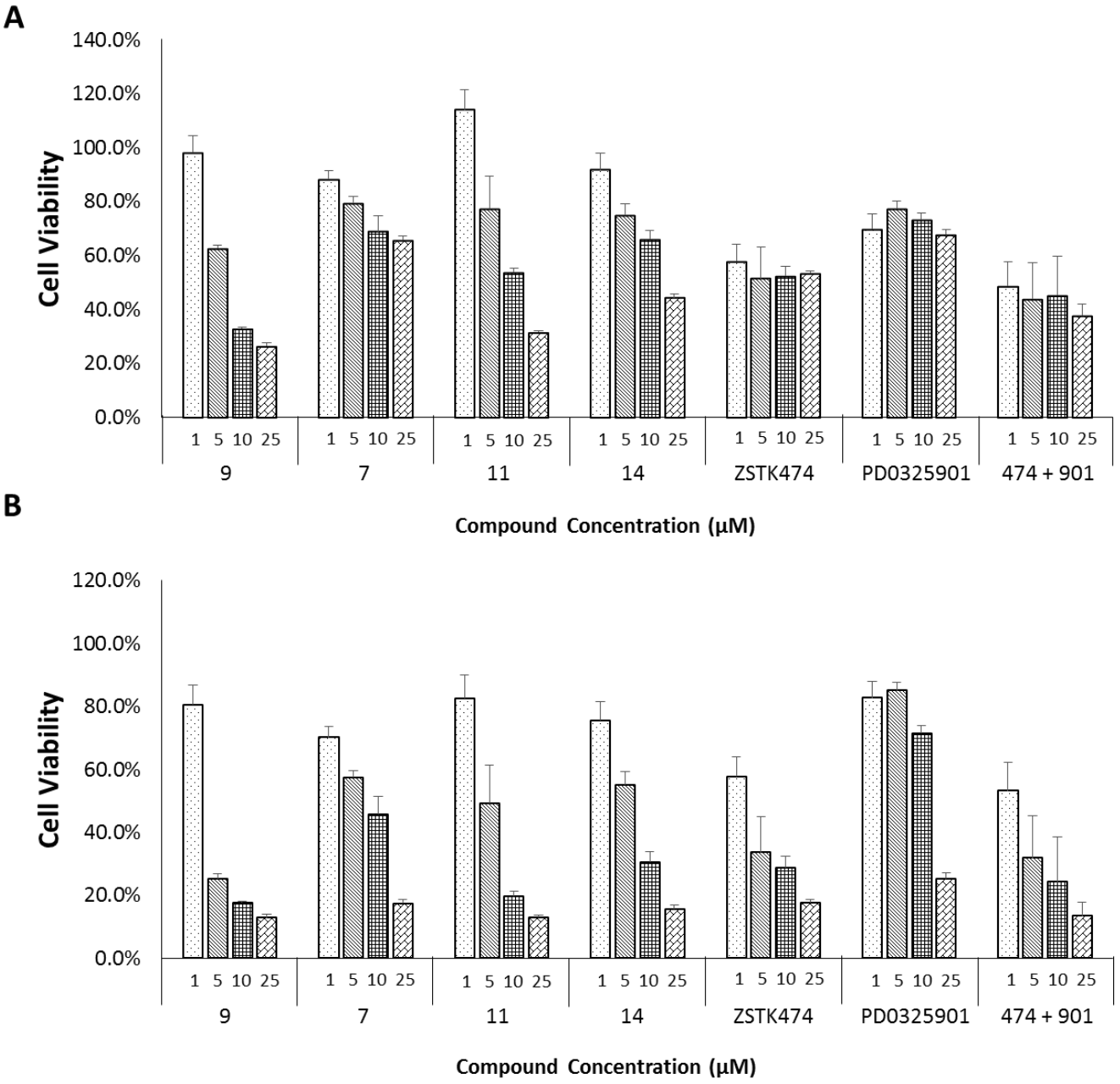
A
140.0%
120.0%
100.0%
80.0%
60.0%
40.0%
20.0%
0.0%
Cell Viability
1 5 10 25
9
7
11
14
ZSTK474
PD0325901
474 + 901
Compound Concentration (μM)
B
120.0%
100.0%
80.0%
60.0%
40.0%
20.0%
0.0%
Cell Viability
1 5 10 25
9
7
11
14
ZSTK474
PD0325901
474 + 901
Compound Concentration (μM)

Figure 7

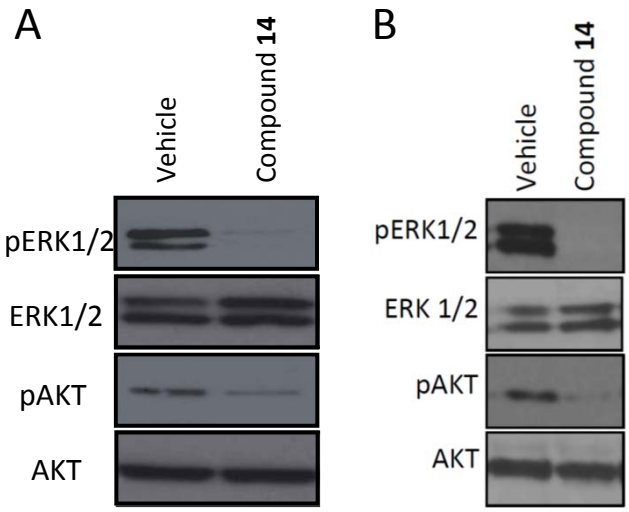
A
Vehicle
Compound 14
pERK1/2
ERK1/2
pAKT
AKT
B
Vehicle
Compound 14
pERK1/2
ERK 1/2
pAKT
AKT